


Cite this: *RSC Adv.*, 2020, 10, 41022

# Synthesis of a super-absorbent nanocomposite hydrogel based on vinyl hybrid silica nanospheres and its properties†

Mingyang Chen,<sup>✉</sup> Yong Shen,<sup>\*</sup> Lihui Xu,<sup>\*</sup> Guanghong Xiang and Zhewei Ni

Superabsorbent polymers as soft materials that can absorb water have aroused great interest in the fields of agriculture and forestry. Water absorption and water retention performance of a hydrogel are important indicators to evaluate its practical application. However, few reports show that hydrogels have both excellent water absorption and water retention properties. To date, superabsorbent hydrogels with a swelling capacity of more than 3000 g g<sup>-1</sup> have rarely been reported. In this work, a novel superabsorbent poly(acrylic acid) (PAA)-based nanocomposite hydrogel (NC gel) was prepared *via* free radical polymerization of acrylic acid by using vinyl hybrid silica nanospheres (VSNPs) as the cross-linking agent. The PAA NC hydrogel achieved a great swelling ratio of more than 5000 times in deionized water at 323 K, and the swollen hydrogel could hold 60% moisture when it was exposed to the air at 303 K for 42 h. Moreover, the hydrogel also obtained a good swelling ratio of 136 g g<sup>-1</sup> in NaCl solution. The PAA NC hydrogel showed excellent repetitive swelling ability. The influences of variable factors (acrylic acid, initiator and sodium hydroxide) on the swelling ratio of the NC hydrogel were researched. It can be speculated that the PAA NC hydrogel has potential application in agriculture and forestry areas due to its excellent water absorption and water retention properties.

Received 17th August 2020  
Accepted 5th November 2020

DOI: 10.1039/d0ra07074b

rsc.li/rsc-advances

## 1. Introduction

Superabsorbent hydrogels (SAH) as a new type of polymer with a three-dimensional network structure that can absorb a lot of water have been widely studied.<sup>1,2</sup> Due to its excellent water absorption performance, SAH are extensively applied in various industries, such as soil amendment, the construction industry, responsive materials and wastewater treatment.<sup>3–7</sup> Especially in agriculture and forestry, SAH can be employed as water-retaining agents to improve soil water retention.<sup>8,9</sup> To date, many novel superabsorbent polymers have been developed, such as double network hydrogel,<sup>10–12</sup> ring slip structure hydrogel, topology structure hydrogel, nanocomposite hydrogel,<sup>13–18</sup> but cannot satisfy the current actual production demand. The main reasons are that these existing hydrogels lack good swelling ratio and water control performance. Therefore, it is urgent to design a novel hydrogel with high water absorption performance and water retention capacity for meeting the needs of industrial development. According to related reports,<sup>19</sup> acrylic polymer shows high hydrophilicity due to a large number of hydrophilic groups on their molecular

chains, which can greatly improve the swelling of hydrogels. Hu *et al.* prepared a novel poly(acrylic acid) (PAA)-based nanocomposite (NC) hydrogel by using calcium hydroxide (Ca(OH)<sub>2</sub>) nanosphere with a diameter less than 5 nm as cross-linker, and the NC hydrogel obtained a good swelling capacity (500 g g<sup>-1</sup>).<sup>20</sup> Tally *et al.* prepared a porous absorbent by grafting poly(acrylic acid-co-acrylamide) onto the sodium alginate backbone, which showed a maximal swelling capacity of 1078 g g<sup>-1</sup>.<sup>21</sup> Shah *et al.* prepared a super absorbent hydrogel with acrylic acid (AA) and acrylamide (AM) *via* single step free radical polymerization, and its SR could reach up to 1841 g g<sup>-1</sup>.<sup>22</sup> However, few literatures reported that the PAA-based hydrogel adsorbents with a swelling ratio (SR) exceeded 3000 g g<sup>-1</sup>. This defect can be attributed to the lack of suitable cross-linking agents.<sup>23</sup> An extremely increased swelling property and water retention performance of hydrogel may be triumphantly obtained if a new cross-linking agent can be used properly. Thence, the key intention of this project is to mainly improve the swelling property of PAA-based hydrogel by developing a suitable cross-linking agent.

Recently, organic-inorganic hybrid materials have been reported to ameliorate the property of polymer materials due to its dual properties of physical toughness and chemical activity.<sup>24,25</sup> In this work, vinyl hybrid silica nanoparticles (VSNPs) with controllable particle dimension was prepared to effectively increase the swelling property and water retention property of the hydrogel. Through different process conditions, the silica

School of Textile and Clothing, Shanghai University of Engineering Science, Shanghai, 201620, PR China. E-mail: shenyong@sues.edu.cn; xulh0915@163.com; Tel: +86-21-67791242

† Electronic supplementary information (ESI) available. See DOI: 10.1039/d0ra07074b



nanospheres with different sizes from 30 nm to 1000 nm were creatively prepared,<sup>26,27</sup> which were employed as a novel cross-linker for poly(acrylic acid) PAA nanocomposite (NC) hydrogel. The design principle of the hydrogel is to graft acrylic acid molecules on the surface of silica nanospheres,<sup>28</sup> forming a three-dimensional network structure. The structures of the superabsorbent PAA NC hydrogel were characterized by TEM, SEM, XRD, EDS, and FT-IR. This work may effectively provide a new design concept for developing super hydrogel absorbents with increased SR and WRR, which may be widely used in agriculture and forestry areas.

## 2. Materials and methods

### 2.1. Materials

Acrylic Acid (AA), sodium dodecyl benzenesulfonate (SDBS), vinyltriethoxysilane (VTES), sodium hydroxide (NaOH), sodium chloride (NaCl), urea ( $\text{CO}(\text{NH}_2)_2$ ), ammonium persulfate (APS) and ammonium hydroxide solution ( $\text{NH}_4\text{OH}$ ) were all purchased from Macklin Chemical Reagent Co. Ltd.

### 2.2. Preparation of VSNPs

The synthesis of VSNPs was mainly through an optimized sol-gel method. The synthesis process was as follows: the measured SDBS was dissolved in deionized water (30 mL), and then VTES of 3.8 mL was added into mixed solution. After two hours, the measured ammonia was added to the mixed liquor at 50 °C. The prepared nanospheres were further purified through at least 5

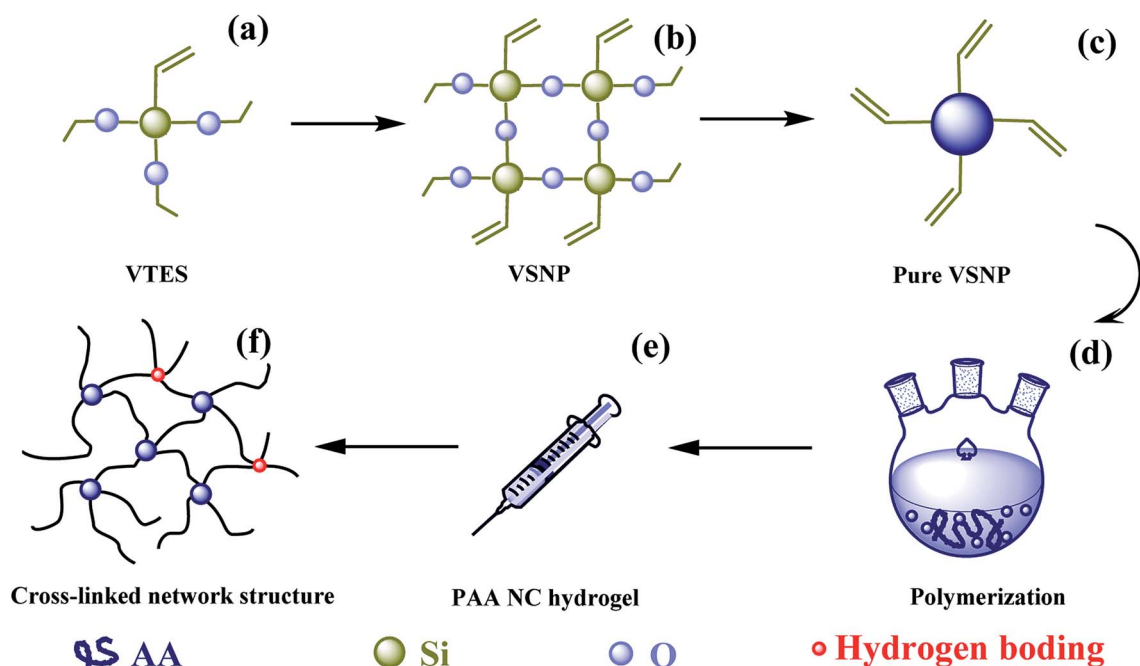
cycles of centrifugation and dispersion. The as-obtained purified VSNPs were dried for further use.<sup>26</sup>

### 2.3. Preparation of PAA NC hydrogel

The above purified VSNPs were used as crosslinking agents for the synthesis of the PAA NC hydrogel. The PAA hydrogel was prepared through a free radical polymerization of AA monomer and VSNPs. Initially, the measured NaOH was dissolved in three-necked flask filled with 20 mL of deionized water at 0 °C. And then, 10 mL of AA monomer and the weighed VSNPs were added into the mixed solution under magnetic stirring. The above process was carried out under  $\text{N}_2$  atmosphere. After two hours, the measured APS was added into the mixed solution, and then the mixed solution was sealed in a syringe. Finally, the PAA NC hydrogel was successfully prepared at 50 °C for 25 h.

### 2.4. Characterization

The shape and size of the VSNPs were characterized by transmission electron microscopy (TEM). Scanning Electron Microscope (SEM, ZEISS MERLIN Compact) was used to characterize the surface morphology of the internal structure of the freeze-dried PAA NC hydrogel. The elements of the VSNPs and the PAA NC hydrogel was individually detected by employing Energy-Dispersive Spectroscopy (EDS). Fourier transformed infrared (FT-IR) spectra of the VSNPs and hydrogel samples were recorded on a Thermo Nicoletis10 FT-IR Spectrometer *via* employing KBr pellets. X-ray diffraction (XRD) patterns of



**Scheme 1** Schematic diagram of PAA hydrogel. (a) VTES was added into SDBS solution; (b) VSNP was synthesized through the hydrolysis and polycondensation of VTES by using the sol-gel method; (c) pure VSNP was obtained through 3 centrifugation processes. (d) Pure VSNPs and AA were dispersed in NaOH solution with strong stirring under  $\text{N}_2$  atmosphere; (e) the above mixed solution is sealed in a syringe and immersed in water at 50 °C for 25 h; (f) formation of the cross-linked structure network diagram of the PAA NC hydrogel employing VSNPs as crosslinking agent.



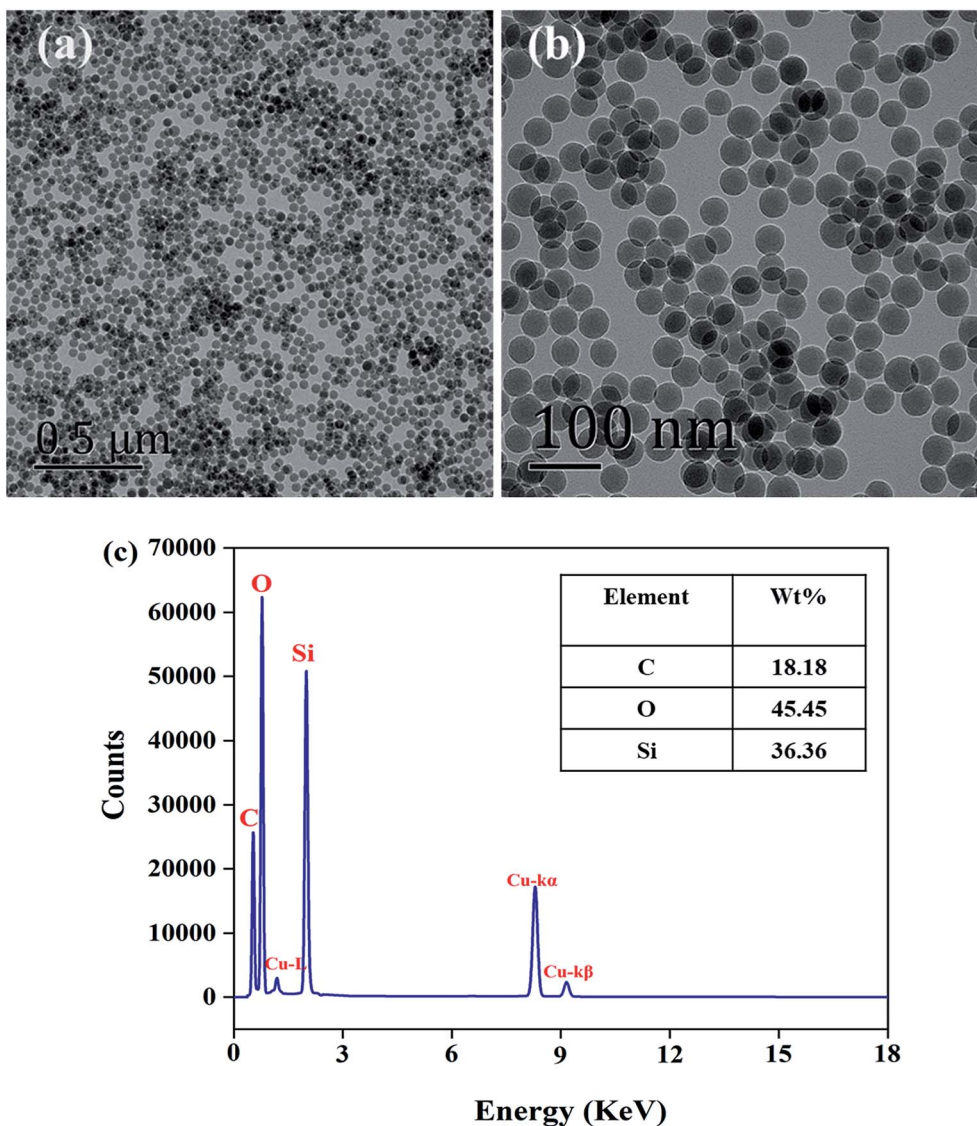


Fig. 1 (a and b) the TEM images of VSNPs, (c) the EDS spectra of VSNPs.

VSNPs and dried hydrogel sample were recorded by using Cu-K $\alpha$  radiation.

$$SR(g\ g^{-1}) = \frac{W_t - W_d}{W_d} \quad (1)$$

## 2.5. Swelling measurements of the PAA NC hydrogel

In this work, the swelling performance of the obtained PAA NC hydrogels was systematically studied under different external environments, including temperature, pH, NaCl and CaCl<sub>2</sub> solutions. Firstly, the hydrogel sample was cut into regular cube shape with size about 5 mm  $\times$  5 mm  $\times$  5 mm, and then the sheared hydrogel sample was dried and recorded the weight ( $W_0$ ). Secondly, the dried hydrogel sample was immersed in the prepared solution until it reached swelling equilibrium. During which time, the swollen hydrogel sample was taken out from the solution to record the weight ( $W_t$ ) at a preset interval and  $W_d$  refers the weight of dried hydrogel. The ultimate swelling ratio (SR) of the PAA NC hydrogel can be calculated as the following formula: (1)

## 2.6. Water retention measurements of the PAA NC hydrogel

The water retention performance of the PAA NC hydrogel was tested at 303 K with humidity around 50%. The swollen PAA NC hydrogel sample was placed in a Petri dish to achieve swelling equilibrium, and the surface area of the hydrogel samples were exposed to the air. The weight of the hydrogel sample was weighted at specified time interval. The water retention ratio of the PAA NC hydrogel was calculated as the following formula: (2)

$$WRR = \frac{W_t - W_d}{W_0 - W_d} \times 100\% \quad (2)$$

where  $W_t$  means the weight of the swollen hydrogel sample at  $t$  time,  $W_d$  refers the weight of the dried hydrogel sample and  $W_0$  is the initial weight of swollen hydrogel sample.



**Table 1** The different sizes of VSNPs under different synthetic conditions

VTES/mL	NH <sub>4</sub> OH/mL	SDBS/mmol	VSNPs average size/nm
3	0.5	1.2	29 ± 4
4	0.5	1.2	30 ± 3
5	0.5	1.2	78 ± 5
4	0.5	0.96	190 ± 7
4	0.5	0.72	257 ± 8
4	0.5	0.48	566 ± 13
4	2	1.2	866 ± 21
4	1	1.2	567 ± 16
4	0.8	1.2	324 ± 10
4	0.2	1.2	126 ± 6

### 3. Results and discussion

#### 3.1. Mechanism of the PAA NC hydrogel formation

In this design, a novel super-adsorbent PAA NC hydrogel was successfully developed by using VSNPs as crosslinking agent. Scheme 1 shows the formation mechanism of the hydrogel. Firstly, VSNPs was the key to the preparation of the hydrogel, because the different sizes of VSNPs would cause different SR of the PAA NC hydrogel. The synthesis principle of VSNPs can be divided into two steps (Scheme 1a and b):<sup>29</sup> (1) VTES hydrolyzes formed silanol bonds in SDBS solution, and then (2) VSNPs were formed by the self-condensation of silanol bonds. Scheme 1c shows the purified VSNPs, which corresponds to the real photograph (Fig. 1a and b). Secondly, the mixed solution of pure VSNPs and AA were added to the three-necked flask to remove oxygen under continuous nitrogen flow (Scheme 1d). After the oxygen was exhausted, the mixed solution was sealed in a syringe for undergoing polymerization of AA and VSNPs (Scheme 1e). Scheme 1f shows the stable physical cross-linked network of the hydrogel, forming by grafting PAA chains on the surface of the VSNPs. Moreover, a mass of hydrophilic groups on the acrylic chains can form hydrogen bonding with each other,<sup>20</sup> which can form a second cross-linking node inside

the hydrogel. The double cross-linked structure of the hydrogel can provide enough stress to allow the hydrogel to fully swell in water. Even under high temperature (323 K) conditions, it can still reach a swelling ratio of more than 5000 times without collapse (ESI Fig. S1a†).

#### 3.2. Single variable reaction condition on the synthesis of VSNPs

The size and dispersion of the VSNPs play a non-negligible role in the synthesis of the hydrogel. Here we mainly focus the factors on VTES, ammonia and SDBS. In the process, ammonia as a catalyst can significantly promote the progress of the polycondensation reaction and SDBS acts as a template container for VSNPs generation. The different synthetic conditions are shown in Table 1. According to Fig. 2, smaller nanospheres can build a well cross-linking density inside the NC gel and improve its SR. Therefore, it can be concluded that the optimal solution for the additive parameters is VTES (4 mL), NH<sub>4</sub>OH (0.5 mL), SDBS (1.2 mmol). As shown in Fig. 1a and b, the TEM images show a regular round appearance and uniform size about 30 nm of VSNPs and proves its good dispersion. The uniform distribution of VSNPs in water without agglomeration is the primary condition for the preparation of high-performance PAA NC hydrogel. EDS analysis (Fig. 1c) shows the content distribution of Si, O, C elements, which is in line with their theoretical distribution values.<sup>29</sup>

#### 3.3. Single variable reaction condition on the SR of the PAA NC hydrogel

In order to prepare a novel adsorbent NC hydrogel with the best swelling ratio, the influence of different monomer variables on the SR of the PAA NC hydrogel was studied individually, and the other variables were set as the optimal reaction conditions.

**3.3.1 Effect of VSNPs size and content.** The content and size of the VSNPs have a great influence on the crosslink density of the PAA NC hydrogel. Network diagram of the PAA NC hydrogel is shown in Scheme 2. Acrylic polymer chains are grafted on the surface of the VSNPs through covalent cross-

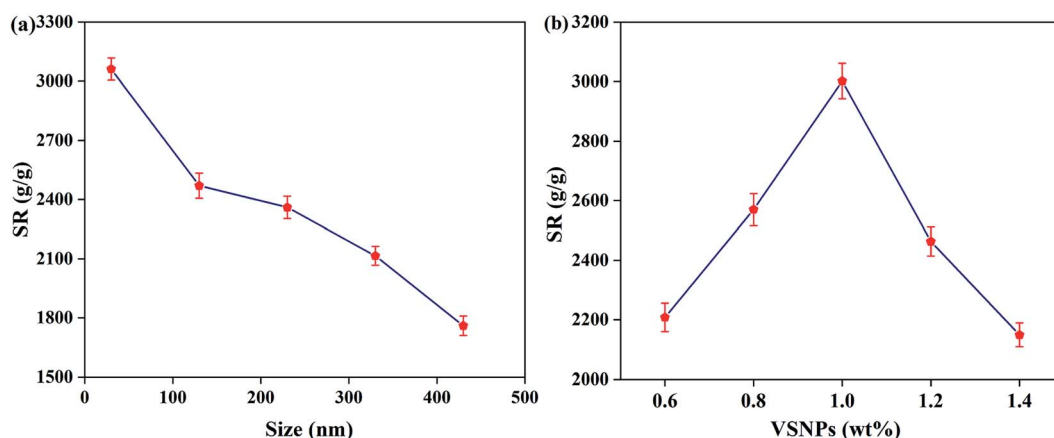
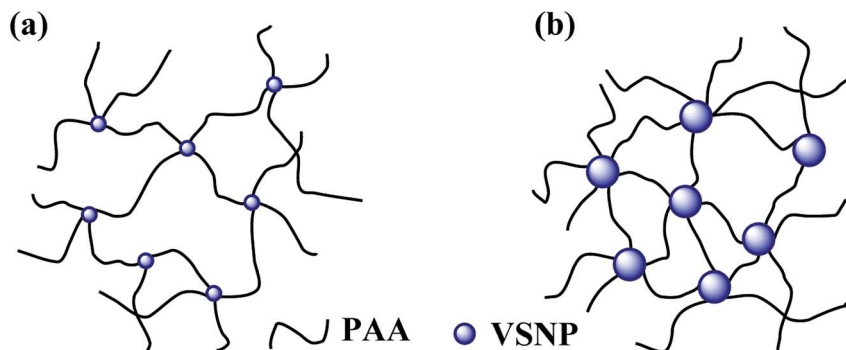


**Fig. 2** (a) SR of the PAA NC hydrogel with different sizes and (b) the concentration of the VSNPs in pure water at 303 K.







Scheme 2 A network structure diagram of different crosslink density.

linking points. A large amount of vinyl groups exists on the surface of the VSNPs, and these vinyl groups increase with the increase of the size. In theory, the crosslink density of the PAA NC hydrogel can be improved by the two ways: (1) increasing the size of the microsphere and (2) increasing the number of VSNPs to obtain more covalent crosslinking points for improving the crosslinking density, resulting in satisfactory SR of the PAA NC hydrogel. However, Fig. 2a shows that the smaller size has better SR at the same quality of nanospheres and the SR reaches the

maximum value when the size is about 30 nm. Whether the nanospheres with smaller size have the same pattern remains to be explored. This phenomenon indicates that the smaller crosslinking agent is more conducive to dissipating the stress of the polymer chains, thereby ensuring that the hydrogel will not collapse when it is fully swollen. The result also echoes the theory that smaller nanoparticles can effectively increase the crosslink density of the hydrogel.<sup>30</sup> Under the condition of the size is about 30 nm, the SR of the PAA NC hydrogel can achieve

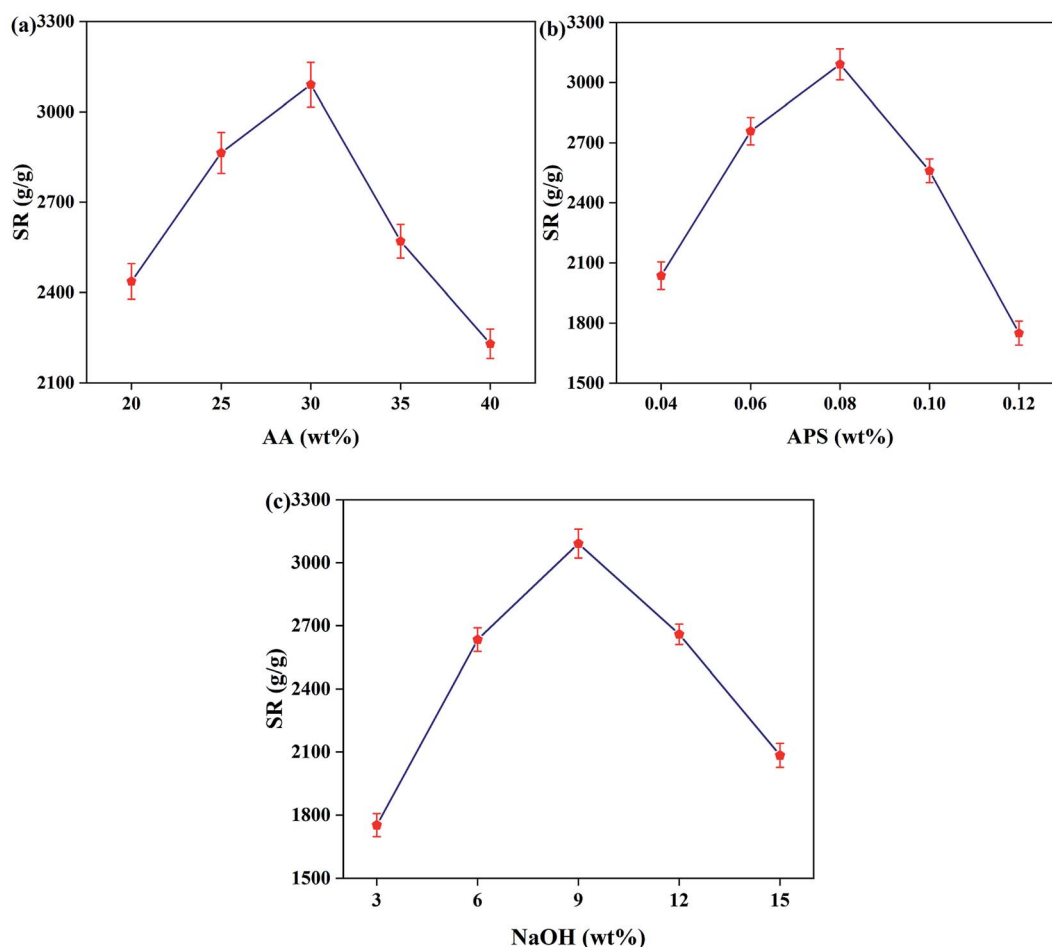


Fig. 3 SR of the PAA NC hydrogel with different content of (a) AA, (b) APS, (c) NaOH.



a maximum value of  $3056 \text{ g g}^{-1}$  at 303 K when the concentration of VSNPs is 1.0 wt% (Fig. 2b). The covalent cross-linking points inside the hydrogel is insufficient when the content of the VSNPs is less than 1 wt%. This situation will cause the hydrogel to partially dissolve during the swelling process. It can be clearly stated that excess or insufficient cross-linking agent could result in poor cross-linking density. Thence, the selection of moderate cross-linking agent is the key to prepare the high swelling ratio NC hydrogel.

**3.3.2 Effect of AA content.** The impact of AA content on SR is shown in Fig. 3a. With the AA content increasing, the SR of the hydrogel shows a trend of increasing and then decreasing. When the content of AA increases from 20 wt% to 30 wt%, the SR of the NC hydrogel increases due to the decrease in cross-linking density. However, when the content of AA exceeds 30 wt% and continues to increase, the crosslinking density will decrease consistently, which causes partial dissolution of the NC hydrogel in water.<sup>31</sup> Therefore, when the concentration of AA is 30 wt%, the PAA NC hydrogel can achieve the best cross-linking density and the maximum SR.

**3.3.3 Effect of APS content.** Fig. 3b shows the influence of initiator content on the SR. It can be found that the SR of the

PAA NC hydrogel increases as the content of the initiator increases when the content of APS is low, and then the SR begins to decrease when the SR reaches a maximum value of  $3056 \text{ g g}^{-1}$ . As the content of initiator increases, more free radicals will form, as will the graft sites, leading to an increase in the SR. However, excessive initiator will reduce the SR of the NC hydrogel due to the excess radicals, leading to a sharp acceleration of the polymerization ratio of AA monomer. Therefore, this situation would reduce the length of AA polymer chains, resulting in a poor SR of the PAA NC hydrogel.<sup>32,33</sup>

**3.3.4 Effect of NaOH content.** As shown in Fig. 3c, NaOH as a reagent that can adjust the degree of neutralization of the solution, showing a great effect on the swelling ratio of the PAA NC hydrogel. Excessive acidity will accelerate the polymerization ratio, leading to an uncontrolled reaction process and creating a chaotic cross-linked network structure. Therefore, as the concentration of NaOH increases, a large number of carboxyl groups in the solution are neutralized, reducing the acidity of the solution. In addition, the electrostatic repulsion between polymer chains inside the PAA NC hydrogel is increased, thereby increasing the SR of the NC hydrogel. However, when the concentration of NaOH exceeds 9%, a large

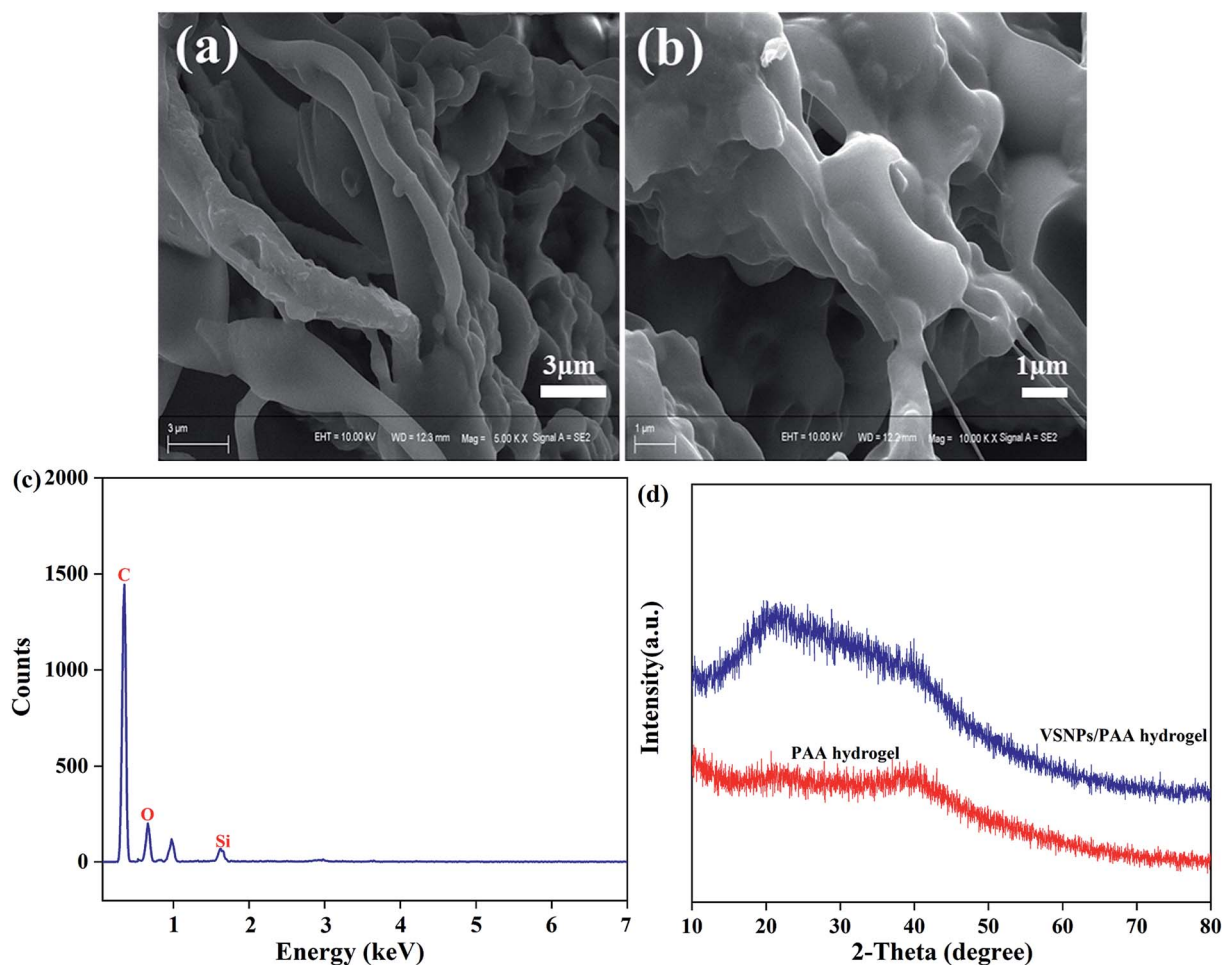


Fig. 4 (a and b) the SEM micrographs of surface morphology of the freeze-dried swollen hydrogel sample, (c) the EDS spectra and (d) the XRD pattern of the PAA NC hydrogel.

amount of  $\text{Na}^+$  will occupy the adsorption sites on the polymer network, reducing the hydrophilicity of the polymer network and decreasing the swelling ratio of the PAA NC hydrogel.<sup>31</sup>

### 3.4. The PAA NC hydrogel structure characterization

The surface morphology of the freeze-dried PAA NC hydrogel was characterized in Fig. 4a and b. It can be intuitively found that the flabby internal morphological structure of the PAA NC hydrogel is composed of these tough branches, and the pore structure inside the hydrogel can act as a storage space for water molecule. These tough branches can effectively distribute the stress to ensure the stability of the network structure when the hydrogel fully absorbs water. Moreover, there are a lot of hydrophilic groups ( $-\text{COOH}$ ) on PAA chains, which can increase the hydrophilicity of the branches, thereby significantly promoting the penetration of water molecules. EDS analysis (Fig. 4c) shows the presence of Si, O, C elements and prove that the extremely low concentration of VSNPs has participated in the polymerization of the PAA NC hydrogel. XRD patterns of the hydrogel samples were displayed in Fig. 4d. The XRD pattern of the dried PAA hydrogel shows a weak peak at  $39^\circ$ , which is caused by the partially crystalline structure of the NC gel. The crystalline structure of the NC gel was attributed to the strong intermolecular and intramolecular hydrogen bonds of the acid molecular chains.<sup>20</sup> Apparently, the peak at  $22^\circ$  of the PAA NC hydrogel is attributed to the introduction of VSNPs.<sup>34</sup> This peak shift illustrates that the addition of the VSNPs can improve the crystallinity of the PAA hydrogel and increase the crosslink density of the PAA hydrogel. However, excessive content of VSNPs will lead to excessive crystallinity of the hydrogel, resulting in a low swelling ratio of the PAA hydrogel in water. Therefore, the high swelling ratio of the PAA hydrogel can be obtained by the introduction of the appropriate content of VSNPs.

To better confirm the preparation of the PAA NC hydrogel, some typical functional groups were studied by FT-IR, as shown

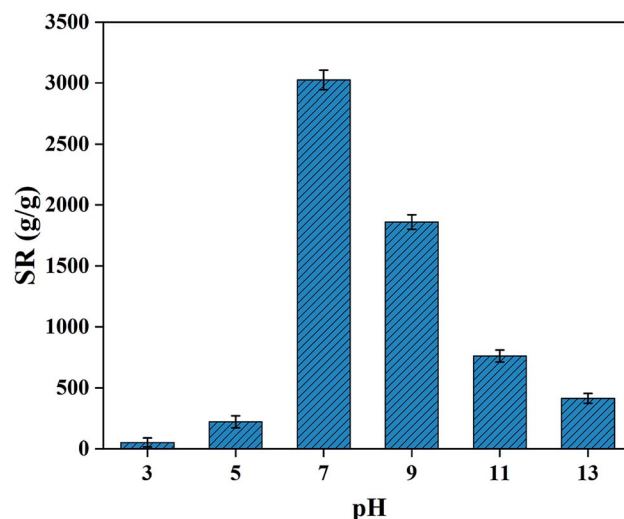


Fig. 6 SR of the PAA NC hydrogel in deionized water with different pH at 303 K.

in Fig. 5. The peak at  $1050\text{ cm}^{-1}$  of  $\text{SiO}_2$  was ascribed to the stretching vibration of  $\text{Si-O-Si}$ . In VSNPs spectra, the two weak peaks at ( $1148\text{ cm}^{-1}$  and  $1048\text{ cm}^{-1}$ ) of VSNPs were the asymmetry structure of  $\text{Si-O-Si}$  and the peak at  $1603\text{ cm}^{-1}$  was ascribed to the stretching vibration of  $\text{C}=\text{C}$ .<sup>35,36</sup> The above characteristic peaks proved the successful synthesis of VSNPs. In the spectrum of the PAA NC hydrogel, the peak at  $1666\text{ cm}^{-1}$  was the stretching vibration of  $\text{C}=\text{O}$  and the peak at  $1489\text{ cm}^{-1}$  was assigned to anti-symmetric vibration of  $-\text{COO}^-$ . The two weak peaks at  $1112\text{ cm}^{-1}$  and  $1095\text{ cm}^{-1}$  were the asymmetry structure of  $\text{Si-O-Si}$  in the PAA NC hydrogel spectra. The stretching vibration of  $\text{C}=\text{C}$  appears at  $1603\text{ cm}^{-1}$  in VSNPs spectra, but it did not appear in the PAA NC hydrogel spectra, certifying that  $\text{C}=\text{C}$  has participated in polymerization. Notably, the peaks at  $1698\text{ cm}^{-1}$ ,  $1452\text{ cm}^{-1}$  and  $1404\text{ cm}^{-1}$  of PAA hydrogel shift to  $1666\text{ cm}^{-1}$ ,  $1489\text{ cm}^{-1}$  and  $1406\text{ cm}^{-1}$  of

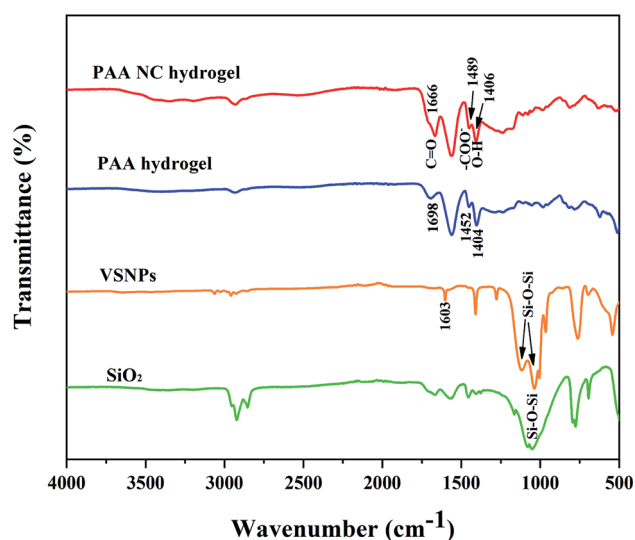


Fig. 5 FTIR spectra of VSNPs, PAA hydrogel and the PAA NC hydrogel.

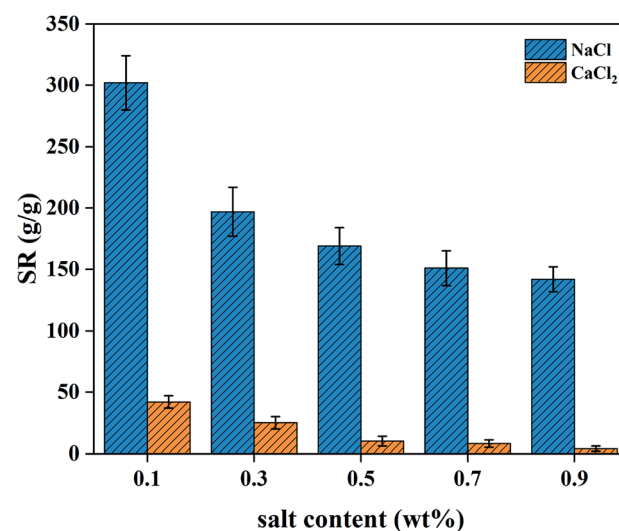


Fig. 7 SR of the PAA NC hydrogel in NaCl and  $\text{CaCl}_2$  solutions at 303 K.



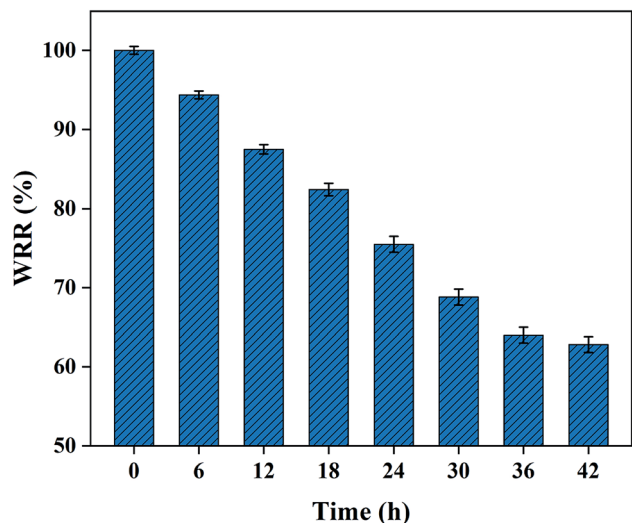


Fig. 8 Water retention of the swollen PAA NC hydrogel at room temperature (303 K) with humidity around 50%.

the PAA NC hydrogel respectively, resulting from the introduction of VSNPs. These characteristic absorption peaks strongly prove that the PAA NC hydrogel has been successfully synthesized in this work.

### 3.5. The PAA NC hydrogel property research

**3.5.1 Swelling in buffer solution.** The water absorption property of the PAA NC hydrogel is extremely sensitive to pH, and the SR was studied at 303 K in buffer solution. The buffer solution with different pH value from 3 to 13 was neutralized by HCl and NaOH. The pH-dependent swelling behaviors are shown in Fig. 6, which illustrates two different trends under acidic and alkaline conditions. This rapid changes in the swelling behavior of this PAA NC hydrogel is related to ionization of the  $-\text{COOH}$  groups on acrylic chains inside the hydrogel. Under acidic conditions, the large amounts of  $-\text{COOH}$  groups are generated by the protonation of  $-\text{COO}^-$ . The hydrogen bonding power among the COOH groups inside the hydrogel are increased and the electrostatic repulsion between  $-\text{COO}^-$  groups are weakened, which can increase the hydrogen bonding crosslink point inside the internal hydrogel network, resulting in poor swelling performance. When the pH value increases, more COOH groups will change into  $-\text{COO}^-$  groups and the electrostatic repulsion of  $-\text{COO}^-$  groups will enhance. Therefore, it can be concluded that the SR will increase with the

increase of pH value from 3 to 7. However, the SR of the PAA NC hydrogel shows a downward trend when the pH from 7 to 13, which can be attributed to the charge shielding effect of  $\text{Na}^+$  counter. Notably, in alkaline solution, more  $\text{Na}^+$  will occupy the active sites with the PH value increases, thereby limiting the anion-anion repulsions and resulting in a poor SR.<sup>23</sup> The optimal SR is obtained when pH is equal to 7, which means that the forces of electrostatic repulsion and hydrogen bonding are in equilibrium.

**3.5.2 Swelling in salt solutions.** The sensitivity of the PAA NC hydrogel to saline and cation were studied in NaCl and  $\text{CaCl}_2$  solutions. Fig. 7 shows the different SR in the solutions of NaCl and  $\text{CaCl}_2$ . It can be intuitively seen that the SR is significantly reduced and decreased with the increase in the concentration of the same salt solution. This rule can be ascribed to a charge shielding effect of excess cations, which causes a reduced osmotic pressure difference between the polymer network and the solution, leading to a poor water absorption performance.<sup>26</sup> Notably, under the same concentration, the PAA NC hydrogel achieved a worse swelling capacity in  $\text{CaCl}_2$  solution. It can be attributed to the formation of water-insoluble calcium carboxylate.

**3.5.3 Water retention property.** The water retention performance of hydrogel is an important indicator to evaluate its practical application property. The water retention performance of the as-obtained PAA NC hydrogel was investigated at 303 K with the humidity of the air around 50%. As shown in Fig. 8, the water retention of the swollen PAA NC hydrogel gradually decreases as time increases. It can still maintain a water content of 60% or more after been exposed to the air at 303 K for 42 h. This satisfactory water retention property is related to its good cross-linked structure and a mass of  $-\text{COOH}$  groups inside the polymer. The good water retention performance depends on the van der Waals force and H-bonding between water molecules and the polymer. Water retention property of this NC hydrogel and other super-absorbent hydrogels are shown in Table 2 for comparing.

**3.5.4 Reswelling ability.** The repeated swelling property of hydrogel is very important in its practical applications. Initially, the swollen PAA NC hydrogel achieved the maximum SR at 303 K, and then it was placed in an oven to remove moisture at 80 °C. The above as-obtained dried hydrogel was used to study the reswelling property. Fig. 9 shows the result of swelling/drying cycle of the PAA NC hydrogel. It can be found that the SR of the NC hydrogel decreased as the times of swelling/drying increased. The result can be mainly attributed to the broken

Table 2 Swelling ratio and water retention property under different factors for reported hydrogel

Hydrogel	Swelling ratio ( $\text{g g}^{-1}$ )	Water retention property (%)	Temperature (K)	Time (d/h)	Reference
CS/PAA	644	29	298	3 d	19
NaAlg/P(AMPS-AA-AM)	822	70	298	6 d	37
PVA-(AA/AM)	1250	65	313	7 h	38
SLS	1328	64	298	6 h	39
VSNPs/PAA	3056	60	303	42 h	This work





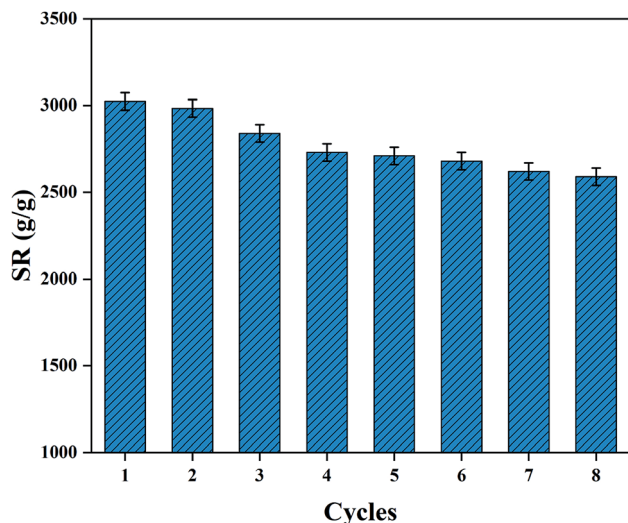


Fig. 9 The reswelling ability of the PAA NC hydrogel in deionized water at 303 K.

cross-linked structure caused by the continuously swelling/drying cycles. Despite this, the SR of the hydrogel can still reach  $2670 \text{ g g}^{-1}$  after conducting the swelling/drying cycles for 8 times. The excellent reswelling ability shows its tough cross-linked skeleton structure inside the hydrogel. The excellent repeated swelling performance can save more cost in its applications, which shows its good application prospects in many biomaterial fields.

## 4. Conclusions

A novel superabsorbent PAA NC hydrogel was successfully prepared by grafting polymerization of acrylic acid onto the surface of vinyl hybrid silica nanospheres *via* free radical copolymerization. The nanospheres build a tough cross-linked network structure inside the hydrogel without the participation of any other cross-linking agent. The chemical structure of the as-obtained PAA NC hydrogel was characterized and verified by TEM, SEM, XRD, EDS and FT-IR. The different variable factors affecting the swelling ratio of hydrogels were systematically studied, such as VSNPs, AA, NaOH and APS. The hydrogel can achieve a SR of  $3056 \text{ g}$  and  $136 \text{ g g}^{-1}$  in deionized water and 0.9% NaCl solution, respectively. In addition, the hydrogel also shows excellent water retention and repeated swelling properties. Thus, the PAA NC hydrogel has huge potential practical application in terms of soil water retention agent of agriculture and forestry.

## Conflicts of interest

The authors declared no conflict of interests.

## Acknowledgements

Funding: the research was supported by National Natural Science Foundation of China (51703123), Talent Program of

Shanghai University of Engineering Science, and Shanghai Engineering Research Center for Clean Production of Textile Chemistry (19DZ2253200).

## References

- 1 S. Wang, Z. F. Zhang, L. F. Dong, G. Waterhouse, Q. H. Zhang and L. F. Li, A remarkable thermosensitive hydrogel cross-linked by two inorganic nanoparticles with opposite charges, *J. Colloid Interface Sci.*, 2019, **538**, 530–540.
- 2 F. Kazeminejadfard and M. Hojjati, Preparation of superabsorbent composite based on acrylic acid-hydroxypropyl distarch phosphate and clinoptilolite for agricultural applications, *J. Appl. Polym. Sci.*, 2018, **136**, 47365.
- 3 Y. C. Chen and Y. H. Chen, Thermo and pH-responsive methylcellulose and hydroxypropyl methylcellulose hydrogels containing  $\text{K}_2\text{SO}_4$  for water retention and a controlled-release water-soluble fertilizer, *Sci. Total Environ.*, 2019, **655**, 958–967.
- 4 A. Roy, P. P. Maity, A. Bose and S. Dhara,  $\beta$ -Cyclodextrin based pH and thermo-responsive biopolymeric hydrogel as a dual drug carrier, *Mater. Chem. Front.*, 2019, **3**, 385.
- 5 F. Zhang, H. Ren, G. L. Tong and Y. L. Deng, Ultra-lightweight poly(sodium acrylate) modified TEMPO-oxidized cellulose nanofibril aerogel spheres and their superabsorbent properties, *Cellulose*, 2016, **23**, 3665–3676.
- 6 X. Y. Hu, Y. M. Wang, M. Xu and L. L. Zhang, Development of photocrosslinked sale can composite hydrogel embedding titanium carbide nanoparticles as cell scaffold, *Int. J. Biol. Macromol.*, 2019, **123**, 549–557.
- 7 R. Bardajee, H. S. Ghasdat and C. Vancaeyzeele, Graphene oxide nanocomposite hydrogel based on poly(acrylic acid) grafted onto salep: an adsorbent for the removal of noxious dyes from water, *New J. Chem.*, 2019, **43**, 3572–3582.
- 8 T. G. Liu, L. W. Qian, B. Li, J. Li, K. K. Zhu, H. B. Deng, *et al.*, Homogeneous synthesis of chitin-based acrylate superabsorbents in NaOH/urea solution, *Carbohydr. Polym.*, 2013, **94**, 261–271.
- 9 B. Wilske, M. Bai, B. Lindenstruth, M. Bach, Z. Rezaie, H. G. Frede, *et al.*, Biodegradability of a polyacrylate superabsorbent in agricultural soil, *Environ. Sci. Pollut. Res.*, 2014, **21**, 9453–9460.
- 10 S. Sharma, R. Kumar, P. Kumari, R. N. Kharwar, *et al.*, Mechanically magnified chitosan-based hydrogel as tissue adhesive and antimicrobial candidate, *Int. J. Biol. Macromol.*, 2019, **125**, 109–115.
- 11 M. J. Su, Y. Liu, S. H. Li, Z. P. Fang, B. Q. He, Y. H. Zhang, *et al.*, A rubber-like, underwater superoleophobic hydrogel for efficient oil/water Separation, *Chem. Eng. J.*, 2019, **361**, 364–372.
- 12 R. Gong, J. J. Ye, W. Dai, X. Y. Yan, J. Hu, X. Hu, *et al.*, Adsorptive removal of methyl orange and methylene blue from aqueous solution with finger-citron-residue-based activated carbon, *Ind. Eng. Chem. Res.*, 2013, **52**, 14297–14303.



- 13 W. M. Cheng, X. M. Hu, Y. Y. Zhao, M. Y. Wu, Z. X. Hu and X. T. Yu, Preparation and swelling properties of poly(acrylic acid-co-acrylamide) composite hydrogels, *e-Polymers*, 2017, **17**, 95–106.
- 14 H. J. Dai and H. H. Huang, Enhanced Swelling and Responsive Properties of Pineapple Peel Carboxymethyl Cellulose-g-poly(acrylic acid-co-acrylamide) Superabsorbent Hydrogel by the Introduction of Carclazite, *J. Agric. Food Chem.*, 2017, **65**, 565–574.
- 15 W. Wang, L. F. Li, Z. J. Li, S. Y. Guo and G. X. Sun, Environmentally Stable Polymer Gels with Super Deformability and High Recoverability Enhanced by Sub-5 nm Particles in the Nonvolatile Solvent, *J. Polym. Sci., Part B: Polym. Phys.*, 2019, **57**, 713–721.
- 16 G. Y. Zhou, J. M. Luo, C. B. Liu, L. Chu and J. Crittenden, Efficient heavy metal removal from industrial melting effluent using fixed-bed process based on porous hydrogel adsorbents, *Water Res.*, 2018, **131**, 246–254.
- 17 S. X. Dong and Y. L. Wang, Characterization and adsorption properties of a lanthanum-loaded magnetic cationic hydrogel composite for fluoride removal, *Water Res.*, 2016, **88**, 852–860.
- 18 J. Wei, Z. X. Low, R. W. Ou, G. P. Simon and H. T. Wang, Hydrogel-polyurethane interpenetrating network material as an advanced draw agent for forward osmosis process, *Water Res.*, 2016, **96**, 292–298.
- 19 S. X. Fang, G. J. Wang, P. C. Li, R. G. Xin, S. Liu, Y. K. Qin, *et al.*, Synthesis of chitosan derivative graft acrylic acid superabsorbent polymers and its application as water retaining agent, *Int. J. Biol. Macromol.*, 2018, **115**, 754–761.
- 20 X. S. Hu, R. Liang and G. X. Sun, Super-adsorbent hydrogel for removal of methylene blue dye from aqueous solution, *J. Mater. Chem. A*, 2018, **6**, 17612–17624.
- 21 M. Tally and Y. Atassi, Synthesis and characterization of pH-sensitive superabsorbent hydrogels based on sodium alginate-g-poly(acrylic acid-co-acrylamide) obtained *via* an anionic surfactant micelle templating under microwave irradiation, *Polym. Bull.*, 2016, **73**, 3183–3208.
- 22 L. A. Shah, M. Khan, R. Javed, M. Sayed, M. S. Khan, A. Khan, *et al.*, Superabsorbent polymer hydrogels with good thermal and mechanical properties for removal of selected heavy metal ions, *J. Cleaner Prod.*, 2018, **201**, 78–87.
- 23 X. S. Hu, R. Liang, J. Li, Z. P. Liu and G. X. Sun, Mechanically strong hydrogels achieved by designing homogeneous network structure, *Mater. Des.*, 2019, **163**, 107–147.
- 24 M. Zhong, F. K. Shi, Y. T. Liu, X. Y. Liu and X. M. Xie, Tough superabsorbent poly(acrylic acid) nanocomposite physical hydrogels fabricated by a dually cross-linked single network strategy, *Chin. Chem. Lett.*, 2016, **27**, 312–316.
- 25 M. Zhong, X. Y. Liu, F. K. Shi, L. Q. Zhang, X. P. Wang, A. G. Cheetham, *et al.*, Self-healable, tough and highly stretchable ionic nanocomposite physical hydrogels, *Soft Matter*, 2015, **11**, 4235–4241.
- 26 M. Y. Chen, Z. W. Ni, Y. Shen, G. H. Xiang and L. H. Xu, Reinforced swelling and water-retention properties of super-absorbent hydrogel fabricated by a dual stretchable single network tactic, *Colloids Surf., A*, 2020, **602**, 125133.
- 27 F. K. Shi, X. P. Wang, R. H. Guo, M. Zhong and X. M. Xie, Highly stretchable and super tough nanocomposite physical hydrogels facilitated by coupling of intermolecular hydrogen bond and analogous chemical crosslinking of nanoparticle, *J. Mater. Chem. B*, 2015, **3**, 1187–1192.
- 28 Y. Huang, M. Zhong, Y. Huang, M. S. Zhu, Z. X. Pei, Z. F. Wang, *et al.*, A self-healable and highly stretchable supercapacitor based on a dual crosslinked polyelectrolyte, *Nat. Commun.*, 2015, **6**, 10310.
- 29 T. S. Deng, Q. F. Zhang, J. Y. Zhang, X. Shen, K. T. Zhu and J. L. Wu, One-step synthesis of highly monodisperse hybrid silica spheres in aqueous solution, *J. Colloid Interface Sci.*, 2019, **329**, 292–299.
- 30 A. Pourjavadi, A. M. Harzandi and H. Hosseinzadeh, Modified carrageenan 3. Synthesis of a novel polysaccharide-based superabsorbent hydrogel *via* graft copolymerization of acrylic acid onto kappa-carrageenan in air, *Eur. Polym. J.*, 2014, **40**, 1363–1370.
- 31 Q. Y. Lv, M. Wu and Y. Shen, Enhanced swelling ratio and water retention capacity for novel super-absorbent hydrogel, *Colloids Surf., A*, 2019, **583**, 123972.
- 32 J. W. Chen and Y. M. Zhao, Relationship between water absorbency and reaction conditions in aqueous solution polymerization of polyacrylate superabsorbents, *J. Appl. Polym. Sci.*, 2000, **65**, 808–814.
- 33 Y. Bao, J. Z. Ma and N. Li, Synthesis and swelling behaviors of sodium carboxymethyl cellulose-g-poly(AA-co-AM-co-AMPS)/MMT superabsorbent hydrogel, *Carbohydr. Polym.*, 2011, **84**, 76–82.
- 34 M. I. H. Mondal, M. S. Yeasmin and M. S. Rahman, Preparation of food grade carboxymethyl cellulose from corn husk agrowaste, *Int. J. Biol. Macromol.*, 2015, **79**, 144–150.
- 35 W. Wang and A. Q. Wang, Nanocomposite of carboxymethyl cellulose and attapulgit as a novel pH-sensitive superabsorbent: Synthesis, characterization and properties, *Carbohydr. Polym.*, 2010, **82**, 83–91.
- 36 M. I. Mondal, M. S. Yeasmin and M. S. Rahman, Preparation of food grade carboxymethyl cellulose from corn husk agrowaste, *Int. J. Biol. Macromol.*, 2015, **79**, 144–150.
- 37 N. Mohammad, Y. Atassi and M. Tally, Synthesis and swelling behavior of metal-chelating superabsorbent hydrogels based on sodium alginate-g-poly(AMPS-co-AA-co-AM) obtained under microwave irradiation, *Polym. Bull.*, 2017, **74**, 4453–4481.
- 38 X. H. Wang, H. Q. Hou, Y. J. Li, Y. Y. Wang, C. Hao and C. W. Ge, A novel semi-IPN hydrogel: preparation, swelling properties and adsorption studies of Co(II), *J. Ind. Eng. Chem.*, 2016, **41**, 82–90.
- 39 X. H. Wang, Y. Y. Wang, S. F. He, H. Q. Hou and C. Hao, Ultrasonic-assisted synthesis of superabsorbent hydrogels based on sodium lignosulfonate and their adsorption properties for Ni<sup>2+</sup>, *Ultrason. Sonochem.*, 2018, **40**, 221–229.

